The International Journal of Advanced Manufacturing Technology (2018) 98:657–669
https://doi.org/10.1007/s00170-018-2299-9

ORIGINAL ARTICLE

Study on optimal independent variables for the thermal error model of CNC machine tools

Xian Wei[1,2] · Feng Gao[1] · Yan Li[1] · Dongya Zhang[1]

Received: 30 January 2018 / Accepted: 5 June 2018 / Published online: 14 June 2018

Abstract
In the technology of thermal error compensation for CNC machine tools, it is particularly important to select modeling variables which can stably reflect the relationship between temperature field and thermal expansion in terms of modeling. This paper analyzes the theories and experiments on the thermal properties of the temperature-sensitive points distributed on one-dimension pole. It is found that the prediction model performs better in prediction accuracy and robustness when established with linear points as independent variables than with nonlinear ones. However, because of the complicated structure of machine tools, it is rather hard to fix the positions of linear points, which consequently lead to the proposal of a comprehensive temperature-feature extraction method that uses feature extraction algorithm and weight optimization to construct linear temperature-sensitive points. Experimental facilities verified the feasibility of its proposal. What's more, based on the effectiveness of building linear measuring points, it is proposed to arrange the temperature sensors along the deforming direction. With the feeding system of a gantry machine tool as the testing platform, the thermal error model established according to the proposed method is actually tested under different working conditions. The result shows this proposed method has higher prediction precision and robustness.

Keywords CNC machine tool · Temperature-sensitive point · Thermal error · Model variable · Thermal properties · Feature extraction

1 Introduction

During the precision finishing process of CNC machine tools, thermal error has become one of the main reasons for the less precise manufacture of parts, accounting for 50~70% of the entire manufacturing error of a machine tool [1, 2]. Now, the impact caused by thermal error can be lessened through many ways, such as the symmetric design in structure, the use of materials with low thermal expansion coefficient, the temperature control in workshops, and the thermal error compensation [3], where thermal error compensation has been regarded as the most cost-effective method.

In the technology of thermal error compensation, the core point is to build up a thermal error model with excellent performance in prediction accuracy and robustness, which, however, critically depend on the selection and arrangement of temperature-sensitive points.

At present, temperature-sensitive points are selected and optimized through firstly laying out many temperature sensors on the machine tool according to engineering experience and then using finite-element analysis or the statistical analysis to pick out a few temperature sensors for modeling. M.H. Attia et al. [4], for example, used finite element analysis to analyze the temperature field of the entire machine tool. The temperature field was divided into many regular units. In this way, the positions and quantity of sensitive points were worked out according to the simulation of temperature field and the correlation between units. However, finite element method is greatly restricted in application because of the great difficulty in defining its boundary conditions. Lo et al. [5] from the University of Michigan realized the selection and optimization of sensitive points through correlation analysis, group-based

✉ Xian Wei
110801844@qq.com

✉ Feng Gao
gf2713@126.com

[1] Key Lab of NC Machine Tools and Integrated Manufacturing Equipment of the Education Ministry & Key Lab of Manufacturing Equipment of Shanxi Province, Xi'an University of Technology, No. 5 Jinhua South Road, Xi'an 710048, China

[2] School of Transportation and Automotive Engineering, Panzhihua University, No. 5 Airport Road, Panzhihua 617000, China

searching, and optimizing. Jiri Vyroubal [6] divided a machine tool into several parts, each of which was correspondingly equipped with a temperature sensor. Finally, the error prediction model was established according to the temperature-sensitive points which were found to be the most related to thermal error through correlation analysis. Using the minimum residual sum of squares as the evaluation function, Lee et al. [7] picked up the temperature-sensitive points efficiently after the sensitive points were optimized by the combination of linear regression and relational analysis. For modeling optimization, Yang et al. [8, 9] adopted gray relational analysis method to screen out the top five temperature-sensitive points by calculating and comparing their gray correlation between thermal error and temperature sensor. Since the gray correlation and fuzzy clustering have an advantage in sensitive point classification and optimization, other researchers also studied them [10, 11]. To avoid the impact caused by the multicollinearity among temperature-sensitive points. Miao et al. [12, 13] optimized modeling variables by principal-component method, which achieved quite a favorable effect on the testing machine tool. By Wang et al. [14], the 20 temperature sensors distributed on the machine tool were selectively optimized through fuzzy clustering method, by which three measuring points were finally chosen as the variables for modeling. However, according to the analysis in literature [12], the optimal measuring points were found variable along with the changes of working conditions during the air cutting experiment on the Leaderway-V450 machine tool. Therefore, the great difference between the actual and modeling working conditions caused by improper temperature-sensitive points will lead to a terrible performance of the thermal error prediction model in accuracy and robustness [15]. With the spindle of a machine tool simplified to a one-dimension pole, Yang et al. [16] located linear sensitive points at the position of about 0.4 L of the slender pole after theoretical and experimental analysis, which, however, leaves out of consideration that some dynamic changes of a machine tool-like heat source strength and contact thermal resistance may cause the position shift of linear measuring points. With the awareness that the dynamic changes of a machine tool may influence its robustness, Xia et al. [17] simplified the ball screw to a one-dimension pole and made theoretical and experimental analysis on dynamic thermal characteristics, showing that there is "advancement" and "hysteresis" between temperature-sensitive points and thermal deformation. After the analysis on the thermal dynamic deformation of one-dimension poles, Yang et al. [18] from the University of Michigan built up the model directly with the information collected from temperature-sensitive point, which, however overlooked the influence caused by multicollinearity.

What's more, with the increasing machining of large parts, the thermal error of the feeding system on large-sized machine tools has captured plenty of attention [19, 20]. But a large machine tool requires a great number of sensors to get the accurate information of temperature field because of its size. For that reason, this paper focus on the thermal error of the feeding system on large-sized machine tools, aiming to solve two problems: (1) at the beginning, try to arrange as few measuring points as possible, as long as the information on temperature variation is certain to be reflected accurately; (2) make sure to establish highly robust models at the selected temperature-sensitive points, when the working conditions of the machine tool are changed.

To solve the problems mentioned above, some basic hypotheses have to be considered: if an approximate linear relation can be found between measuring point and thermal error, the thermal-property identification model will be able to have its accuracy and robustness greatly improved and its difficulty greatly reduced, because of the favorable interpolation and extrapolation performances of linear prediction models.

To prove the above hypothesis, the lead screw was simplified to be a one-dimensional pole in this paper, so as to realize theoretical analysis by analytical method and finite difference method. According to the analyzing result, the linear relation indeed exists between a sensitive point and its thermal expansion. However, because of the complicated structure, the machine tool is simultaneously influenced by the contact thermal resistances among different surfaces, which makes it rather hard to find this measuring point immediately. Therefore, this paper put forward a temperature-feature extraction method to construct this linear measuring point, which was verified on the feeding system of a gantry machine tool. Experimentally comparing with a model which was established on the basis of fuzzy clustering and gray correlation method, the thermal prediction model proposed in this paper is proved to be more effective in prediction.

2 Analysis for thermal expansion

The thermal error of feeding system originates from the heat generation when the ball screw is running. For that reason, it is necessary to conduct some analysis on the entire heat transmission of feeding system before the thermal error is studied. Ball screw feeding system is shown as Fig. 1 where the left bearing is used to fasten the ball screw and the right bearing only offers support to the ball screw rather than stop its movement from side to side. The motor and bearings are the main heat source for ball screw feeding system. Therefore, ball screw system can be simplified to be a one-dimensional heated pole structure shown in Fig. 2, if it is assumed as below: (1) the ball screw has an even heat distribution in the redial direction; (2) with the surface grooves neglected, the ball screw is simplified to be a solid rod; (3) the influence of lube on heat transmission is neglected; (4) the contact heat resistances between machinery parts are neglected; (5) the heat exchange

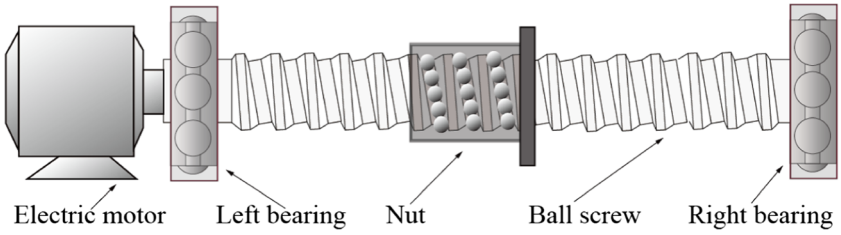

Fig. 1 Sketch of ball screw feeding system

between ball screw and surrounding air is mainly realized by convective heat loss. Small temperature gap between them will lead to low heat exchange which can be neglected. (6) the screw of the gantry machine tool is long enough to avoid the temperature coupling of the two screw ends.

2.1 Theoretical analysis

Shown as Fig. 2, the left end is fastened and the right end is free. L is the pole length. The red arrow in the picture means the running direction of heat. Its differential equation of heat conduction is

$$\frac{k}{\rho c}\frac{\partial^2 T}{\partial x^2}=\frac{\partial T}{\partial t}+\frac{4\alpha_h c_g}{kA}(T-T_a) \tag{1}$$

where k means heat conductivity; ρ refers to the density of ball screw; c means specific heat capacity; $T(x,t)$ is the function of position x and time t, standing for the temperature at some point on the pole; α_h is the synthetic heat release coefficient of air; c_g is the perimeter of cross section; A is the cross section of the pole; and T_a is environment temperature.

$$T(x,0)=T_0 \tag{2}$$

When boundary condition is $x=0$ and $x=L$,

$$\left.\frac{\partial T}{\partial x}\right|_{x=0}=-\frac{q}{kA} \tag{3}$$

where q means heat flux density.

$$\left.\frac{\partial T}{\partial x}\right|_{x=L}=-\frac{h_r}{k}[T(L,t)-T_0] \tag{4}$$

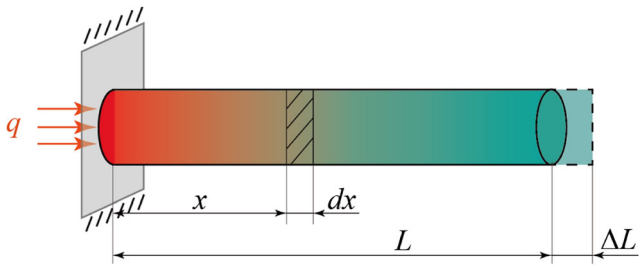

Fig. 2 The simplified one-dimensional model of ball screw

where h_r is the surface heat transfer coefficient per unit area and L is the length of the one-dimensional pole.

The region of definite solutions is divided into a grid by time stepΔt and space step Δx. nodes(x_i, t_j) are shortened to be (i, j) where $x_i = i\Delta x, i = 0,1,\ldots, m$, $\Delta x = {}^{L}/_{m}$, $t_j = j\Delta t$, $j = 0,1,2,\ldots n$. The finite difference equation formulated by CE (group explicit) algorithm [21] is

$$\begin{bmatrix} 1+r & -r & & & & \\ -r & 1+r & \ddots & & & \\ & \ddots & 1+r & -r & & \\ & & -r & 1+r & & \\ & & & & 1+r \end{bmatrix} \cdot \begin{bmatrix} T_1^{j+1} \\ T_2^{j+1} \\ \vdots \\ T_{m-3}^{j+1} \\ T_{m-2}^{j+1} \\ T_{m-1}^{j+1} \end{bmatrix} = \begin{bmatrix} 1-r & & & & & \\ & 1-r & r & & & \\ & r & 1-r & \ddots & & \\ & & \ddots & 1-r & r & \\ & & & r & 1-r \end{bmatrix} \cdot \begin{bmatrix} T_1^{j} \\ T_2^{j} \\ \vdots \\ T_{m-3}^{j} \\ T_{m-2}^{j} \\ T_{m-1}^{j} \end{bmatrix} + b_1 \tag{5}$$

where $T_i^j = T(i,j)$ is the solution of Eq. (1)at the discrete point (i, j), $r = {}^{\Delta t}/_{\Delta x^2}$ is the ratio of mesh, and $b_1 = \left[rT_0^j, 0, \ldots, 0, rT_m^{j+1}\right]$. Taking the mesh size as $\Delta t =$ 1 min and $\Delta x =$ 25 mm, and the mesh number as $n = 180$ and $m = 40$, the temperature rise at a random point can be worked out according Eq. (5) when the material parameters in Table 1 are taken into Eq. (1).

The thermal expansion of the one-dimensional pole can be acquired through Eq. (6)

$$\Delta L = \int_0^L \varepsilon[T(x,t)-T_0]dx \tag{6}$$

Table 1 Material parameters of lead screw

Parameters	Value
k	46.5 w/(m·k)
ρ	7830 kg/m^3
C	443 J/(kg·°C)
α_k	12.5 w/(m^2·°C)
C_g	60 π mm
A	900 π mm

where ε refers to the heat expansion coefficient.

With Eqs. (5) and (6), it is able to calculate the temperature and thermal expansion at a random point on the one-dimensional pole. The correlation curve between them is shown in Fig. 3 where there are totally ten measuring points included. T_1 is close to the heat source and T_{10} is 720 mm away from the heat source. A measuring point is selected every 80 mm to calculate its temperature and thermal expansion which is shown by the curve in Fig. 3. From Fig. 3, the temperature varies faster than thermal expansion at T_1 the closest point to the heat source whose curve is concave; with the measuring point going farther from the heat source, temperature is fading and the curve is consequently getting less concave, which makes the curve of temperature and thermal expansion gradually go linearly just like the curve of T_3 in Fig. 3. At the point of T_4 which is much farther from the heat source, its curve is in a convex shape, which means thermal expansion varies faster than temperature. Therefore, it can be concluded that there must be a point whose curve of temperature and thermal expansion is approximate to a straight line while the thermal error curve is turning from the concave to the convex. This point is called as linear temperature-sensitive point, while other measuring points are called as nonlinear sensitive point.

Besides, the relation between measuring point and thermal expansion of pole under different conditions can be simulated by choosing different heat flux density. With different heat flux densities, the relation curve of temperature and thermal expansion at T_1, T_3, and T_4 can be acquired through Eq. (5) and (6), which is shown as Fig. 4. From Fig. 4(a, c), it can be seen that the relation between temperature and thermal deformation at T_1 and T_4 is nonlinear, and the shape of its thermal error curve also changes as the heat flux density changes, which theoretically reveals the reason [10] why the optimal temperature-sensitive point would be different and the thermal error prediction model would be less robust when working condition changed. However, as Fig. 4(b) shows, when heat flux density changes, there is an approximately linear relation between temperature and thermal deformation at T_3, which is almost unaffected by the changes of heat flux density. Therefore, it can be concluded that when linear measuring points are used as independent variables for modeling, the approximately linear relation between temperature and thermal deformation is able to guarantee the model's robustness no matter how the working condition changes.

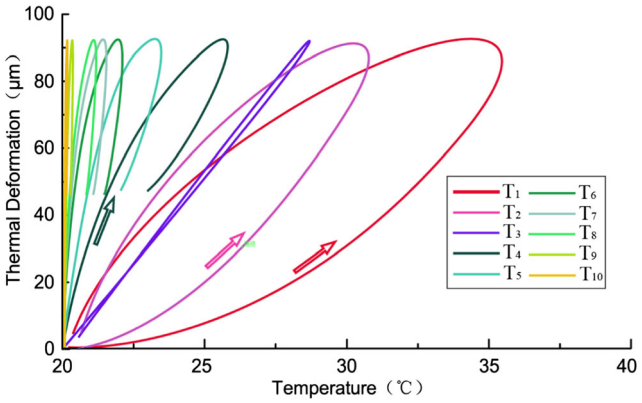

Fig. 3 Curve of temperature and thermal deformation from T_1 to T_{10}

According to the above theoretical analysis on the relations between the temperature and thermal error of the one-dimensional pole, it can be concluded as below: (1) within the limited lengthen of the pole, there must be a sensitive point which is linearly related with thermal error. According to experiment and engineering experience, linear sensitive points are generally distributed within a distance of 400 mm from the heat source; (2) when heat flux density changes, the linear point is still able to keep the linear relation with thermal deformation. Such a linear relation is of strong robustness; (3) the farther the distance from the linear measuring point, the clearer the nonlinear features get.

2.2 Experimental verification

To test the above conclusions of theoretical analysis, the experiment system was designed as Fig. 5 shows. A GCr15SiMn steel rod with the length of 1000 mm was used as the one-dimensional pole in the experiment. One end of the steel rod was fixed on the workbench, while the other end is free; when the left end is heated, a GL-C803 temperature controller was used to realize the heat control by controlling the heating ring, and an ANRITSU METER temperature sensor (E-type MG-24E-GW1-ANP, measurement accuracy is ±0.2 °C) was used to measure the temperature. At the right end, an electric eddy sensor was used to measure the axial deformation of the rod. The model number of this data acquisition instrument is NI-USB-6216.

Heat source intensity was respectively selected to be 12, 1000, and 700 w/m^2·s; temperature rising lasted for 1 h and temperature reduction lasted for 2 h; the temperature measuring points were respectively selected to be 25 mm (T_1), 160 mm (T_3,) and 240 mm (T_4) away from the heat source. The relation curve of measured temperature and thermal deformation is shown as Fig. 6.

By comparing Figs. 4 and 6, it can be seen that theoretical calculation is basically consistent with the experimental result, except for a slight discrepancy that the curve of temperature and thermal expansion in Fig. 6(b) has a better linearity than that in Fig. 4(b). However, when the temperature sensor was moved from 160 to 180 mm, the curve acquired was basically in the same shape of the curve in Fig. 4(b). That means the location of the linear measuring point can be influenced

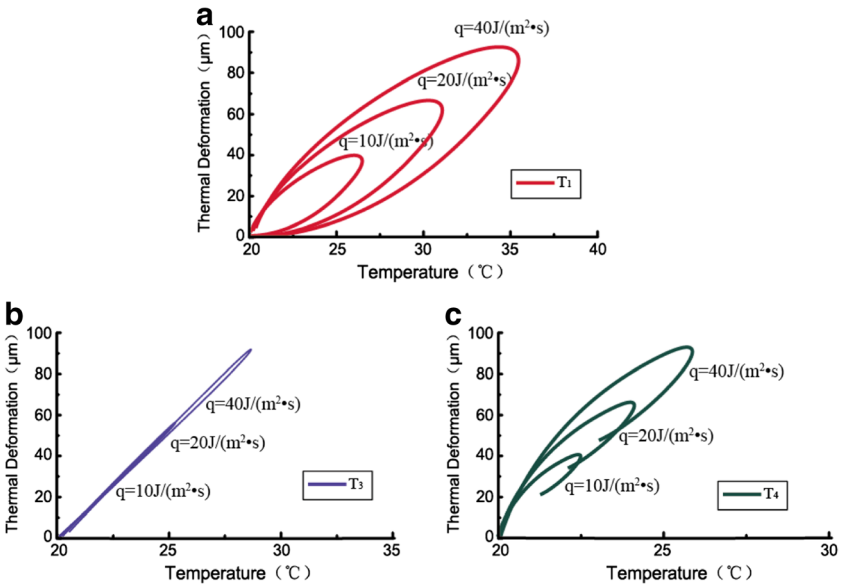

Fig. 4 Curve of temperature and thermal deformation in different heat flux densities

by some factors like the contact thermal resistance between heating ring and metal rod and the control accuracy of the temperature controller. As a result, because of the complicated structure and contacting relations within machine tools, it is actually rather hard to identify the accurate position of the linear measuring point in practice.

Therefore, is it possible to show the temperature features of the linear point by the feature information of the nonlinear points which are classified into a concave group and a convex group according to the different shapes of their thermal deformation curves with temperature changing, so as to construct the thermal error prediction model of high precision and strong robustness. The details will be demonstrated in the following section.

3 Construction of optimal independent variables and temperature sensor layout method

3.1 Variable optimization

For thermal error compensation modeling, it is expected that the most all-sided features of temperature variation can be expressed with a minimum number of independent variables, so that the model operation can be sped up to a certain extent. At the same time, there is always multicollinearity among original temperature-sensitive points, which will influence the prediction accuracy of this model [12]. However, feature extraction algorithm is an effective solution to the problems on the quantitative optimization and multicollinearity of sensitive points.

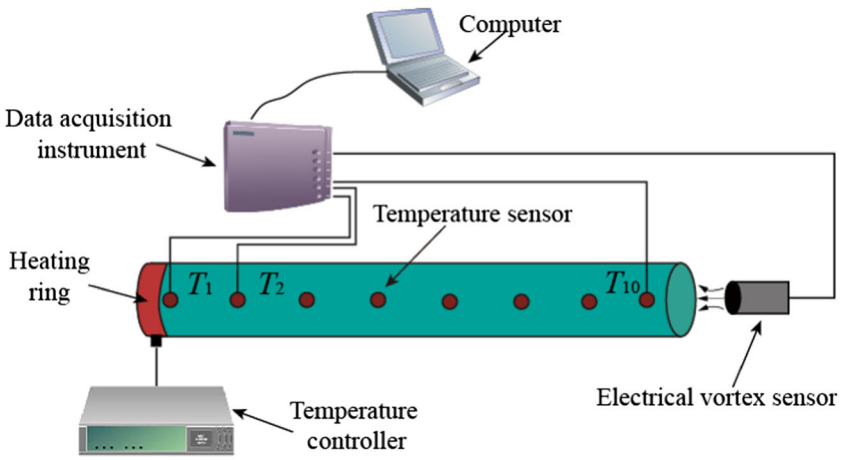

Fig. 5 Composition sketch of experimental system

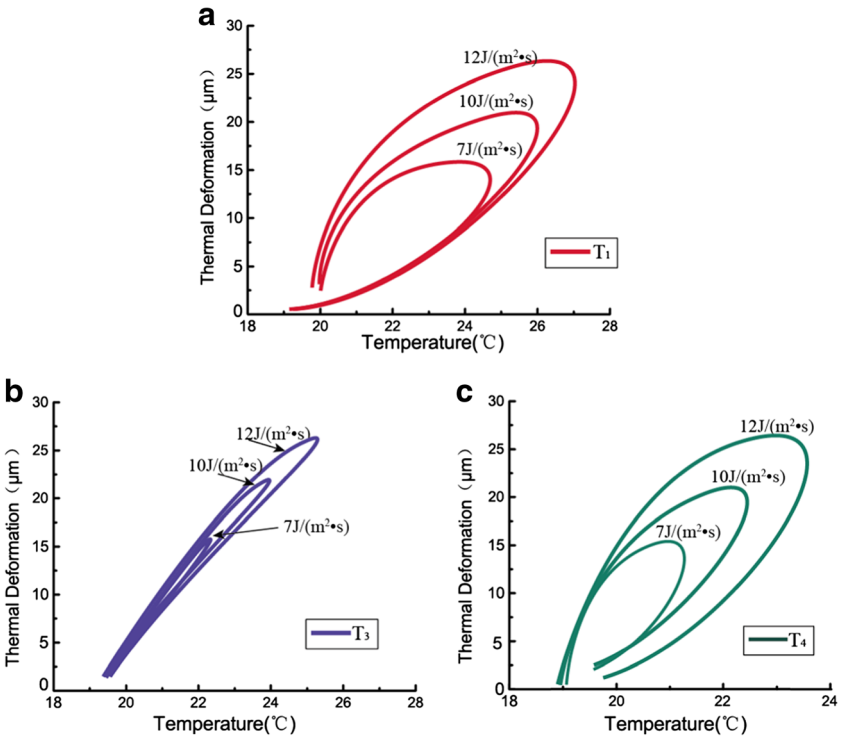

Fig. 6 Relation curves of temperature and thermal deformation at different measuring points

3.1.1 Feature extraction principle

For a multivariable research subject done by statistical analysis technique, too many variables may make the research more complicated. In many cases, temperature variables can be correlated to each other in some way, which also means that the two variables reflected some overlapped information. However, feature extraction principle, as a kind of statistical approach, changes a group of possibly related variables into a group of linear unrelated ones with orthogonal transformation, by which a relatively minimum number of new unrelated variables will be produced by cutting out some unnecessary repeated variables (closely related variables). And these new variables will reflect the original temperature information as much as possible.

3.1.2 Feature extraction algorithm

Set the temperature variable as

$$\boldsymbol{X} = \left(\boldsymbol{x}_1, \boldsymbol{x}_2, \cdots, \boldsymbol{x}_p\right)^T \tag{7}$$

Its n groups of measured valued are expressed as

$$\boldsymbol{x}_i = \left[\boldsymbol{x}_{i1}\ \ \boldsymbol{x}_{i2}\cdots\boldsymbol{x}_{ip}\right]^T,\ \ i = 1, 2, \cdots, n \tag{8}$$

(1) The structure of sample matrix

$$\boldsymbol{X} = \begin{bmatrix} \boldsymbol{x}_1^T \\ \boldsymbol{x}_2^T \\ \vdots \\ \boldsymbol{x}_n^T \end{bmatrix} = \begin{bmatrix} \boldsymbol{x}_{11} & \boldsymbol{x}_{12} & \cdots & \boldsymbol{x}_{1p} \\ \boldsymbol{x}_{21} & \boldsymbol{x}_{22} & \cdots & \boldsymbol{x}_{2p} \\ \vdots & \vdots & \cdots & \vdots \\ \boldsymbol{x}_{n1} & \boldsymbol{x}_{n2} & \cdots & \boldsymbol{x}_{np} \end{bmatrix} \tag{9}$$

where $\boldsymbol{x}_{ij}$ represents the jth variable value among the temperature data in group i.

(2) After conversing the sample matrix $\boldsymbol{X}$, the calculation arrives at $\boldsymbol{Y} = [\boldsymbol{y}_{ij}]_{n \times p}$, where

$$\boldsymbol{y}_{ij} = \begin{cases} \boldsymbol{x}_{ij} \\ -\boldsymbol{x}_{ij} \end{cases} \tag{10}$$

where $\boldsymbol{x}_{ij}$ refers to positive index and $-\boldsymbol{x}_{ij}$ refers to inverse index.

(3) After $\boldsymbol{Y}$ is transformed by standardization, the calculation arrives at

$$\boldsymbol{Z} = \begin{bmatrix} \boldsymbol{z}_1^T \\ \boldsymbol{z}_2^T \\ \vdots \\ \boldsymbol{z}_n^T \end{bmatrix} = \begin{bmatrix} \boldsymbol{z}_{11} & \boldsymbol{z}_{12} & \cdots & \boldsymbol{z}_{1p} \\ \boldsymbol{z}_{21} & \boldsymbol{z}_{22} & \cdots & \boldsymbol{z}_{2p} \\ \vdots & \vdots & \cdots & \vdots \\ \boldsymbol{z}_{n1} & \boldsymbol{z}_{n2} & \cdots & \boldsymbol{z}_{np} \end{bmatrix} \tag{11}$$

where

$$z_{ij} = \frac{y_{ij} - \bar{y}_j}{s_j} \tag{12}$$

$\bar{y}_j$ and s_j respectively represents the average value and standard deviation of column j in matrix $\boldsymbol{Y}$.

(4) Calculate the sample-relation numerical matrix of the standardized matrix $\boldsymbol{Z}$

$$\boldsymbol{R} = \left[r_{ij}\right]_{p\times p} = \frac{\boldsymbol{Z}^T\boldsymbol{Z}}{n-1} \tag{13}$$

(5) Work out the eigenvalues

$$\left|\boldsymbol{R} - \alpha \boldsymbol{I}_p\right| = 0 \tag{14}$$

by which p eigenvalues are acquired, $\alpha 1 \geq \alpha 2 \ldots \geq \alpha p \geq 0$;

(6) To make the information of temperature feature have a coverage of above 85%, m is determined through:

$$\frac{\sum_{j=1}^{m} \alpha_j}{\sum_{j=1}^{p} \alpha_j} \geq 0.85 \tag{15}$$

For each $\alpha_j j = 1,2,\ldots m$, to solve $Rb = \alpha_j b$, unit vector is expressed

$$b_j^0 = \frac{b_j}{\|b_j\|} \tag{16}$$

(7) Solve the feature component of $z_i = [z_{i1}, z_{i2}, \cdots, z_{ip}]^T$

$$u_{ij} = z_i^T b_j^0, j = 1,\ 2, \ldots, m$$

decision matrix is as follows:

$$U = \begin{bmatrix} u_1^T \\ u_2^T \\ \vdots \\ u_p^T \end{bmatrix} = \begin{bmatrix} u_{11} & u_{12} & \cdots & u_{1m} \\ u_{21} & u_{22} & \cdots & u_{2m} \\ \vdots & \vdots & \cdots & \vdots \\ u_{p1} & u_{p2} & \cdots & u_{pm} \end{bmatrix} \tag{17}$$

Among them, u_i is eigenvector of the ith variable.

3.1.3 Weight optimization of variables

By the extraction of feature variable, two temperature feature variables are acquired from those two kinds of temperatures, so as to finally achieve a comprehensive feature variable which has a linear relation with thermal expansion value. To get that comprehensive feature variable, the abovementioned problem is solved by a constraint optimization problem.

$$\begin{aligned} &\mathrm{Max}(\mathrm{corcoef}(T, E)) \\ &s.t.\ \ T = a \times T_a + b \times T_b \\ &\qquad a + b = 1 \\ &\qquad a \geq 0; b \geq 0 \end{aligned} \tag{18}$$

where coecoef() is a correlation function, T refers to comprehensive temperature feature variable, E is the value of thermal expansion, T_a and T_b are the temperatures of feature extraction after feature extraction algorithm is practiced, and a and b are variable coefficients.

With Eq. (18), the variable coefficients a and b can be acquired by using Lagrange function.

3.1.4 Construction step of optimal independent variable

The optimal independent variable is constructed as Fig. 7 shows. The first step is to get temperature sequence and thermal error sequence through the thermal error test for machine tools; next, the measuring points are to be classified according to their curves of temperature and thermal deformation which are concave or convex; then, the temperature feature for

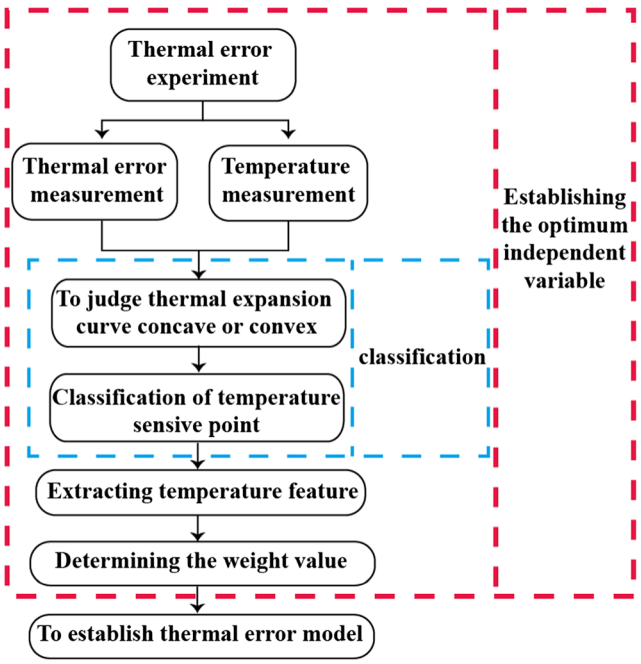

Fig. 7 The modeling process of temperature feature variables

expressing convexity or concavity is extracted by the feature extraction algorithm. The final step is to construct the optimal independent variable.

3.2 Effect of optimal independent variable

In this section, the effectiveness of temperature feature variables is going to be experimentally verified. With the temperature and thermal deformation data acquired when the heat source intensity is 1000 w/m^2, the verification will be conducted in the system shown in Fig. 5. Since T_3 point at the distance of 160 mm has the best linear relation with thermal deformation, this method can be proved effective as long as the linear correlation coefficient between the constructed feature variable and thermal deformation is greater than the correlation coefficient between T_3 and thermal expansion.

Firstly, T_1~T_4 are treated as one group and T_5~T_{10} are treated as the other group based on their curve shape of temperature and thermal deformation: concave or convex.

With Formulas (9)–(14), the feature values of group 1 (T_1–T_4) and group 2 (T_5–T_{10}) are worked out as Tables 2 and 3 show.

With Formula (15), coverage rates are worked out as Tables 2 and 3 show.

According to Tables 2 and 3, both of group 1 and group 2 have their coverage rates of the first features over 85%. Therefore, the first feature components in both groups are used to produce independent variables.

By putting each $\alpha_j (j = 1, 2, \ldots, m)$ shown in Tables 2 and 3 into the formula $Rb = \alpha_j b$, feature vectors can be achieved as below:

$$\boldsymbol{U}_a = [0.375\ 0.089\ 0.101\ 0.215]$$

$$\boldsymbol{U}_b = [0.117\ 0.026\ 0.159\ 0.213\ 0.052]$$

Therefore, the comprehensive feature variable for groups T_1~T_4 is as follows:

$$T_a = 0.375T_1 + 0.089T_2 + 0.101T_3 + 0.215T_4 \tag{19}$$

Table 2 Coverage rate of feature values (group 1)

Feature (j)	Feature value (α)	Coverage (%)
1	4.23	89
2	0.31	7
3	0.21	4

Table 3 Coverage rate of feature values (group 2)

Feature (j)	Feature value (α)	Coverage (%)
1	3.11	86
2	0.24	8
3	0.16	4
4	0.08	2

Similarly, the comprehensive feature variable for groups T_5~T_{10} is as follows:

$$T_b = 0.117T_5 + 0.026T_6 + 0.159T_7 + 0.213T_8 + 0.052T_9 + 0.097T_{10} \tag{20}$$

The two coefficients of the comprehensive temperature feature variables T_a and T_b are worked out with Eq. (18), which are 0.379 and 0.621 respectively. Therefore, the expression for the optimal independent variable is as follows:

$$T = 0.379T_a + 0.621T_b \tag{21}$$

The optimal variable T and the measuring point T_3 are shown in Fig. 8; it is obvious that the optimal independent variable T has a better linear relation than temperature-sensitive point T_3, by which this method is proved to be effective.

3.3 Temperature sensor layout method

A linear measuring point can be constructed with the temperature sequence near the linear measuring point, which means it is feasible to arrange some temperature measuring points along the axis in deforming direction. Therefore, this paper proposed to lay out temperature sensors every 100 to 150 mm along the central axis of deforming direction within a distance of 500 mm from the heat source. The sketch is shown in Fig. 9. This

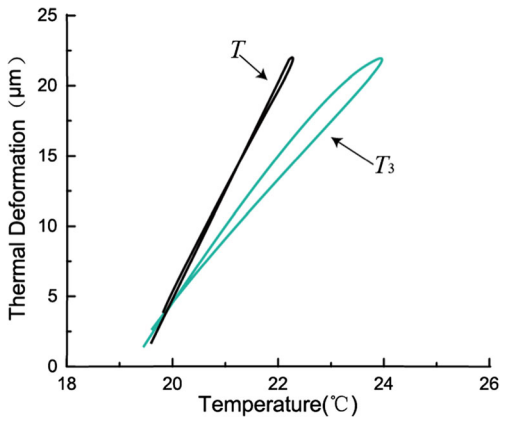

Fig. 8 Linear effect of the optimal independent variable

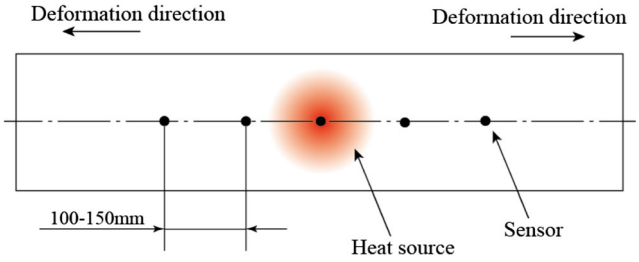

Fig. 9 Sketch of sensor layout method

method overcame the disadvantages of the traditional experiential arrangement by which a large number of sensors were required and arranged disorderly.

4 Experimental verification for modeling effect

The effectiveness of the optimal variable was experimentally verified in previous section. In this section, the thermal error model established according to the proposed method will be further proved to be effective on a gantry machine tool. According to the international standard *Test Code for Machine Tools—Part 3: Determination of Thermal Effects* (IS0 2303:2001 IDT) [22], five batches of thermal error experiment were carried out at specific feed rate and on different seasonal conditions. Prediction accuracy and robustness was analyzed for the thermal error model which was established according to the experimental data. Besides, to verify its superiority, the proposed model was compared with the model optimized by fuzzy clustering theory and gray correlation theory.

4.1 Experimental design

The feeding system of a highly precise gantry five-axis boring-milling machining center was taken as the experimental platform. The machine tool structure is shown in Fig. 10. The temperature sensor from T_1 to T_{10} was used to achieve the temperature data of the feed system. According to the proposed layout method, temperature sensors were installed, the installation position of temperature sensors is shown in Table 4, and the layout of temperature sensors on the machine tool is shown in Fig. 11. Location error was measured by a RenishawXL-80 laser interferometer, whose gauging head is shown as the enlarged view in Fig. 10. In total, five groups of no-load experiments were carried out on the feed system. The running parameters for each group are listed in Table 5.

4.2 Prediction performance analysis

The model was established with the temperature and position error of C_3. And the prediction accuracy and robustness of the model was verified with the data of C_1, C_2, C_4, and C_5.

4.2.1 Optimal independent variable modeling

In this paper, the motor and left bearing in the ball screw feeding system were considered as one heat source which was measured from T_1 to T_6, and the right bearing was considered as the other heat source which was measured from T_7 to T_{10}. For T_1~T_6, the two of the acquired feature independent variables T_{a1} and T_{b1} are

$$\begin{aligned} T_{a1} &= 0.374T_1 + 0.168T_3 + 0.215T_6 \\ T_{b1} &= 0.298T_2 + 0.452T_4 + 0.185T_5 \end{aligned}$$

According to Formula (18), the optimal independent variable can be worked out as below.

$$T_{ab1} = 0.276T_{a1} + 0.724T_{b1} \tag{22}$$

Similarly,

$$\begin{aligned} T_{a2} &= 0.431T_7 + 0.379T_{10} \\ T_{b2} &= 0.3831T_8 + 0.428T_9 \\ T_{ab2} &= 0.362T_{a2} + 0.638T_{b2} \end{aligned} \tag{23}$$

According to the theory on the comprehensive error modeling for feeding system [23, 24],

$$\begin{aligned} E_1 = &\left(3.17 + 0.062\delta_y - 1.87\delta_y^2\right. \\ &\left. + 1.67 \times 10^{-6}\delta_y^3 - 3.65 \times 10^{-9}\delta_y^4\right) \\ &+ \left(-2.31 + 0.124T_{ab1} + 0.059T_{ab2}\right) \times \left(\delta_y - \delta_0\right) \end{aligned} \tag{24}$$

Equation (24) is the thermal error prediction model for feeding system, in which T_{ab1} and T_{ab2} can be worked out through Eqs. (22) and (23), δ_y refers to the y coordinate value of the position where the machine tool is located, and δ_0 refers to the zero point of the y axis in the machine tool coordinate.

4.2.2 Fuzzy clustering and gray correlation modeling

According to fuzzy clustering theory and gray correlation theory, T_1, T_5, T_7, and T_{10}were screened out to be the temperature variables for modeling. Similarly, according to the theory on the comprehensive error

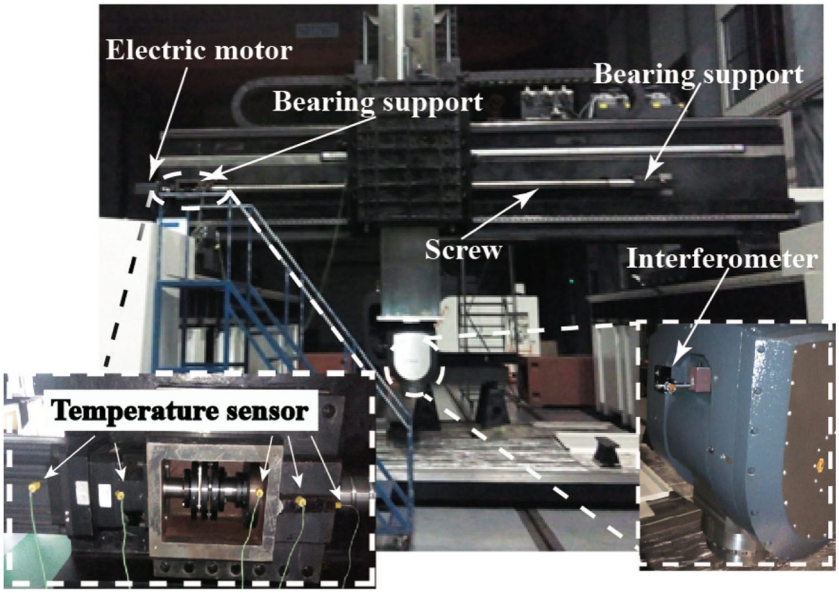

Fig. 10 Structure chart of the testing machine tool

Table 4 Location of temperature sensors on the machine

Location	Sensor numbers
Electric motor	T_1,T_2
Left bearing support	T_3,T_4,T_5,T_6
Right bearing support	T_7,T_8,T_9,T_{10}

modeling for feeding system, fuzzy clustering and gray correlation model is shown as Eq. (25)

$$E_2 = \left(3.17 + 0.378\delta_y + 0.961\delta_y^2 + 3.872 \times 10^{-6}\delta_y^3 - 3.989 \times 10^{-9}\delta_y^4\right) + (2.51 - 0.605T_1 + 0.484T_5 + 0.532T_7 + 0.278T_{10}) \times (\delta_y - \delta_0) \quad (25)$$

In this paper, the optimal independent variable model and the fuzzy-clustering gray-correlation model are respectively represented by Model I and Model II.

4.2.3 Accuracy comparison

According to the experimental data acquired under working condition C_3, the optimal independent variable model (Model I) and the fuzzy-clustering gray-correlation model (Model II) were established. Then, Model I and Model II were respectively used to make predictions for working conditions C_1, C_2, C_4, and C_5. Their prediction effects of forward direction are shown in Fig. 12. Among them, the forecasting effect of C_1 operating condition are shown as Fig. 12(a), the forecasting effect of C_2 operating condition are shown as Fig. 12(b), the forecasting effect of C_4 operating condition are shown as Fig. 12(c), and the forecasting effect of C_5 operating condition are shown as Fig. 12(d).

From Fig. 12(c) and Table 6, it can be seen that the working condition C_3 for modeling is quite similar to the predicted working condition C_4, for which both Model I and Model II have a favorable prediction effect. However, from Fig. 12(a, b, d), and Table 6, it can be seen that when there is a great difference between the predicted and

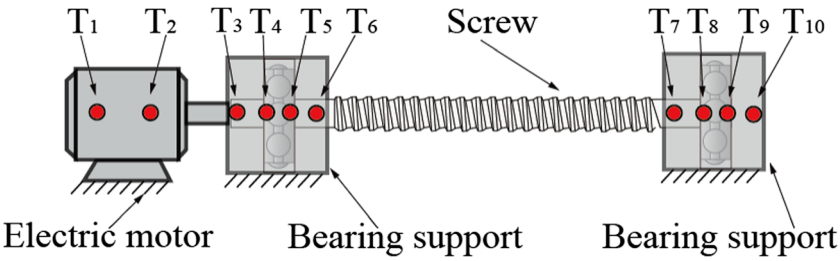

Fig. 11 Layout of temperature sensors in feeding system

Table 5 Experiment parameters

Category	Feed rate (m/min)	Ambient temperature (°C)
C_1	1	5.6–9.8
C_2	1	11.7–17.9
C_3	5	13.4–19.6
C_4	5	18.3–21.5
C_5	10	19.7–23.2

declines slightly. But by contrast, Model II has quite a terrible prediction effect.

The prediction effects of backward direction are shown in Fig. 13 and Table 7. The effects of backward direction are similar to those of the forward direction.

According to the analysis described above, it is shown that when the difference between the modeling and predicted working conditions is slight, both models can have an excellent prediction effect; however, if the working condition during machining is quite different from that for modeling, the modeling working conditions, Model I still has a great performance in robustness, although its prediction accuracy

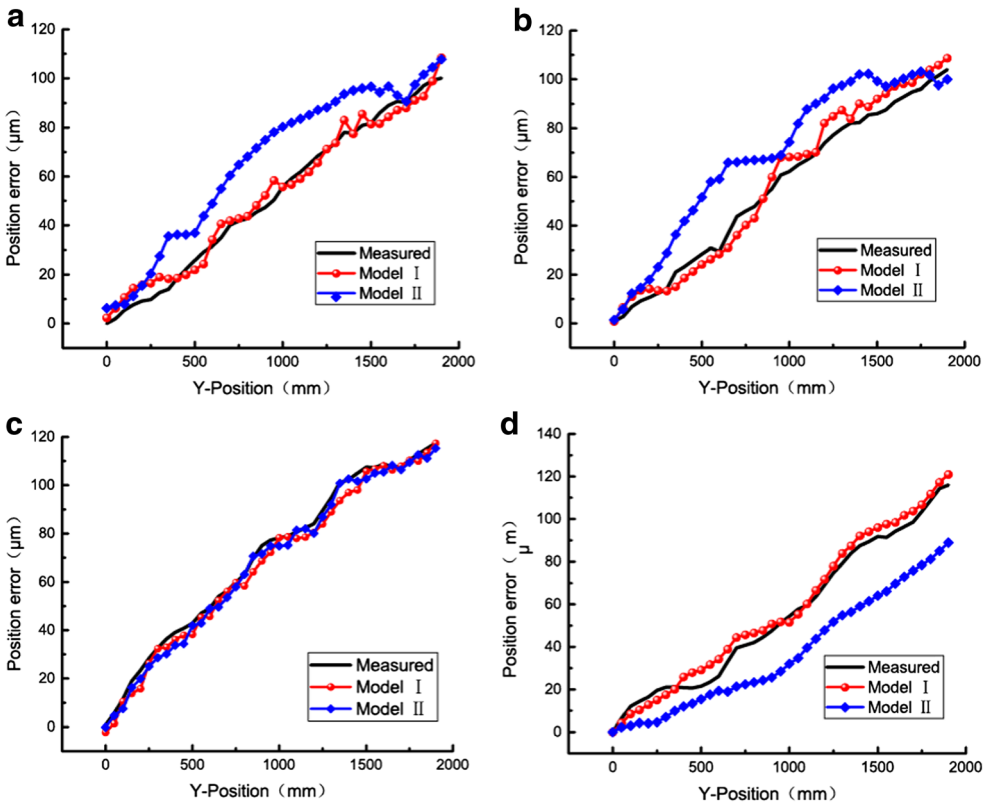

Fig. 12 Effect of forward direction prediction

Table 6 Forecasting accuracy of Model I and Model II (forward direction)

	Standard deviation (μm)		Max-residual error(μm)		Residual sum of squares (μm)	
	Model I	Model II	Model I	Model II	Model I	Model II
C_1	4.12	16.39	8.361	27.78	663	10,478.85
C_2	5.02	16.01	8.29	29.61	986.29	10,000.03
C_4	3.74	3.12	7.524	6.45	545.62	376.01
C_5	4.46	19.99	8.18	29.43	777.89	15,588.21

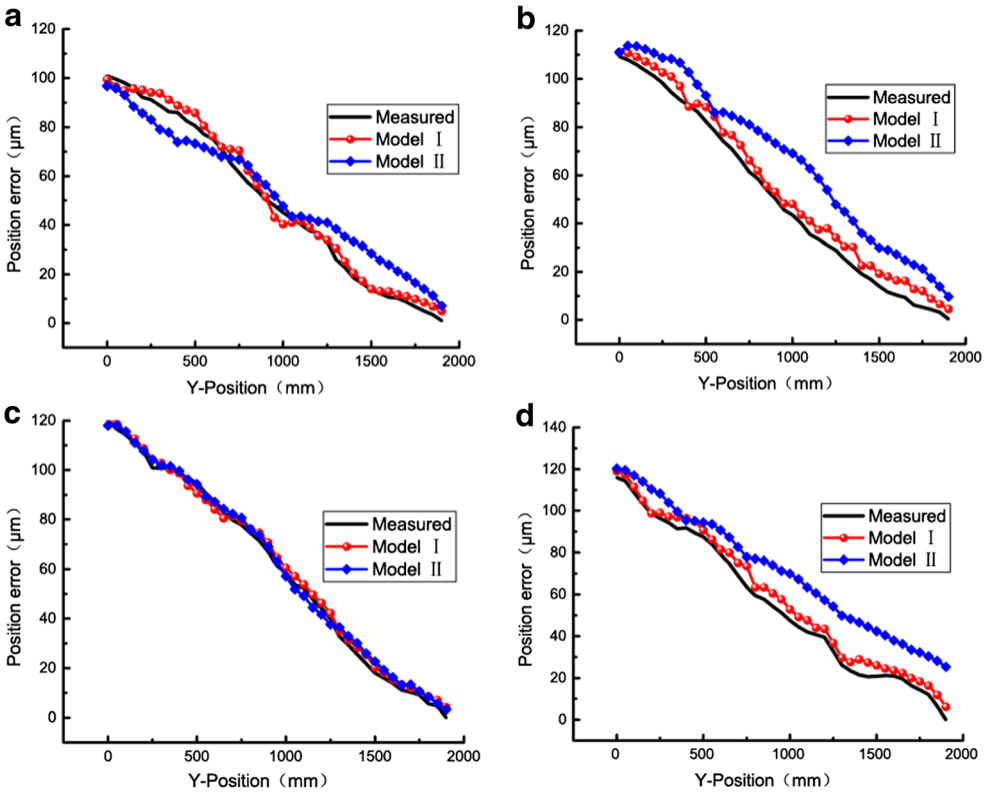

Fig. 13 Effect of backward direction

Table 7 Forecasting accuracy of Model I and Model II (backward direction)

	Standard deviation (μm)		Max-residual error (μm)		Residual sum of squares (μm)	
	Model I	Model II	Model I	Model II	Model I	Model II
C_1	4.07	14.17	7.45	26.63	614	9875.04
C_2	4.98	16.25	8.3	28.29	895.85	9943.03
C_4	3.23	3.11	8.31	6.97	542.31	402.89
C_5	4.55	18.82	7.15	26.56	675.12	9739.87

model proposed in this paper is able to realize high prediction accuracy and robustness.

5 Conclusions

(1) According to the theoretical and experimental analysis on the measuring points on the one-dimensional pole, it was found that there are linear and nonlinear temperature-sensitive points. What's more, along with heat source intensity varying, the linear measuring point has a generally unchanged linear feature on the relation between its temperature and thermal expansion, while the nonlinear measuring points have accordingly varying curves about the relation between temperature and thermal expansion.

(2) Because the construction of linear measuring points is effective, this paper proposed to lay out temperature sensors along the axis of deforming direction, which can, with effect, avoid the large demand on sensor quantity that is caused by disorder arrangement.

(3) A range of air cutting experiments was performed on the feeding system of a highly precise gantry five-axis boring-milling machining center. The results show that the optimal independent variable model has a greater robustness and precision accuracy.

Funding information This study is supported by the National Natural Science Foundation of China (no. 51375382) and the Science and Technology Support Plan Project of Sichuan Province, China (no. 2016GZ0205).

References

1. Bryan J (1990) International status of thermal error research. CIRP Ann Manuf Technol 39:645–656
2. Ramesh R, Mannan MA, Poo AN (2000) Error compensation in machine tools—a review: part II: thermal errors. Int J Mach Tools Manuf 40(9):1257–1284
3. Mayr J, Jedrzejewski J, Uhlmann E, Alkan Donmez M, Knapp W, Härtig F, Wendt K, Moriwaki T, Shore P, Schmitt R, Brecher C, Würz T, Wegener K (2012) Thermal issues in machine tools. CIRP Ann Manuf Technol 61(2):771–791
4. Attia MH, Fraser S (1999) A generalized modelling methodology for optimized real-time compensation of thermal deformation of machine tools and CMM structures. Int J Mach Tools Manuf 39(6):1001–1016
5. Lo CH, Yuan J, Ni J (1999) Optimal temperature variable selection by grouping approach for thermal error modeling and compensation. Int J Mach Tools Manuf 39(9):1383–1396
6. Vyroubal J (2012) Compensation of machine tool thermal deformation in spindle axis direction based on decomposition method. Precis Eng 36(1):121–127
7. Lee JH, Yang SH (2002) Statistical optimization and assessment of a thermal error model for CNC machine tools. Int J Mach Tools Manuf 42(1):147–155
8. Guo Q, Xu R, Yang T, He L, Cheng X, Li Z, Yang JG (2015) Application of GRAM and AFSACA-BPN to thermal error optimization modeling of CNC machine tools. Int J Adv Manuf Technol 83(5–8):995–1002
9. Yao X, Fu J, Xu Y, He Y (2013) Synthetic error modeling for NC machine tools based on intelligent technology. Procedia CIRP 10: 91–97
10. Zhang T, Ye W, Shan Y (2015) Application of sliced inverse regression with fuzzy clustering for thermal error modeling of CNC machine tool. Int J Adv Manuf Technol 85(9–12):2761–2771
11. Yan JY, Yang JG (2009) Application of synthetic grey correlation theory on thermal point optimization for machine tool thermal error compensation. Int J Adv Manuf Technol 43(11–12):1124–1132
12. Miao E, Liu Y, Liu H, Gao Z, Li W (2015) Study on the effects of changes in temperature-sensitive points on thermal error compensation model for CNC machine tool. Int J Mach Tools Manuf 97: 50–59
13. Zhang CX, Gao F, Meng ZH, Zhao BH, Li Y (2015) A novel linear virtual temperature constructing method for thermal error modeling of machine tools. Int J Adv Manuf Technol 80(9–12):1965–1973
14. Wang L, Wang H, Li T (2015) A hybrid thermal error modeling method of heavy machine tools in z–axis. Int J Adv Manuf Technol 80(1–4):389–400
15. Ramesh R, Mannan MA, Poo AN, Keerthi SS (2003) Thermal error measurement and modelling in machine tools. Part II. Hybrid Bayesian network—support vector machine model. Int J Mach Tools Manuf 43:405–419
16. Yang JG, Fan KG (2013) Research on the thermal deformation pseudo-lag and real-time compensation for CNC machine tool spindle. J Mech Eng 49(23):129–135
17. Xia JY, Hu YM, Wu B, Shi TL (2008) Analysis of the thermal dynamic characteristic of machine tools based on unidimensional heat transfer. Mechanical Sci Technol Aeros Eng 27(10):1121–1126
18. Yang H, Ni J (2003) Dynamic modeling for machine tool thermal error compensation. J Manuf Sci Eng 125(2):245–254
19. Liu Q, Yan J, Pham DT, Zhou Z, Xu W, Wei Q, Ji C (2016) Identification and optimal selection of temperature-sensitive measuring points of thermal error compensation on a heavy-duty machine tool. Int J Adv Manuf Technol 85(1–4):345–353
20. Shi H, Ma C, Yang J, Zhao L, Mei XF, Gong G (2015) Investigation into effect of thermal expansion on thermally induced error of ball screw feed drive system of precision machine tools. Int J Mach Tools Manuf 97:60–71
21. Zhang BL, Gu TX, Mo ZY (1999) Principles and methods of numerical parallel computation. National Defense Industry Press, Beijing
22. ISO 230-3 (2001) Test code for machine tool—part 3: determination of thermal effects. ISO copyright office, Geneva
23. Wang W, Yang JG, Yao XD, Fan KG, Li ZH (2012) Synthesis modeling and real-time compensation of geometric error and thermal error for CNC machine tools. Chin J Mech Eng 48(7):165–1709
24. Wei X, Gao F, Li Y, Li YH, Ma Z (2016) Optimization of thermal error model critical point for gantry machine tool feeding system. Chin J Sci Instrum 37(6):1340–1346